Journal of Sound and Vibration (1997) **208**(2), 175–187

EVALUATION OF THE LONGITUDINAL COUPLED VIBRATIONS IN ROTATING, FLEXIBLE DISKS/SPINDLE SYSTEMS

H. S. JIA

System Mechanics Group, Mechanical Engineering Research Laboratory, Korea Electric Power Research Institute, 103-16, *Munji-Dong, Yusung-Ku, Taejon* 305-380, *Korea*

S. B. CHUN

Department of Environmental Engineering, Korea Kyung-In Women's College, 548-4, *Kyesan-Dong, Kyeyang-Ku, Inchon* 407-050, *Korea*

AND

C. W. LEE

Center for Noise and Vibration Control, Department of Mechanical Engineering, Korea Advanced Institute of Science and Technology, Science Town, Taejon 305-701, *Korea*

(*Received* 21 *January* 1997, *and in final form* 14 *May* 1997)

The natural frequencies and modes of the longitudinal coupled vibrations in a flexible shaft with multiple flexible disks are determined through a substructure synthesis technique. The analysis rotor model consists of multiple flexible disks attached to a flexible shaft with varying annular cross-section, as used for steam turbines or computer storage devices. In modelling the system, disk flexibility and centrifugal stiffening effects are taken into account. Commercial computer hard disk drive spindle systems are selected as illustrative examples. In particular, the effects of disk flexibility on the longitudinal coupled vibrations between the shaft and disks are investigated with varying spindle rotational speed. The results indicate that the substructure synthesis technique allows a clear physical insight into the effect of disk flexibility with reasonable computational effort.

1. INTRODUCTION

Analytical solutions to shaft–disk components are generally restricted to flexible shaft–rigid disk models. In this paper, the idealizations are relaxed by introducing disk flexibility. The rotordynamic analysis of the flexible shaft–flexible disk model is intricate due to the presence of coupled vibrations between the shaft and disks. According to the nature of coupling with the rotor, disk vibratory modes may be classified into three groups: uncoupled disk modes with more than one nodal diameter, umberella modes coupled with the shaft longitudinal vibrations and disk modes with a single nodal diameter coupled with the shaft bending vibrations [1]. The importance of disk flexibility on the bending coupled vibrations has been discussed in some works [2–9].

So far, little work has addressed the longitudinal (axial) coupled vibration, but it is of practical importance, in particular, for computer hard disk drive (HDD) spindle systems (Figure 1), since the longitudinal coupled vibration will interact with the read/write head,

0022–460X/97/470175 + 13 $25.00/0/sv971127

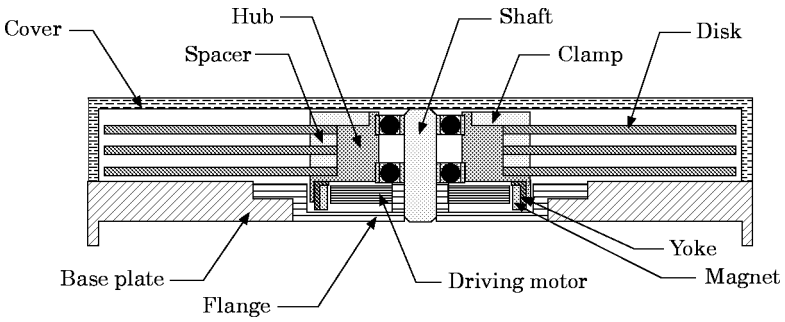

Figure 1. Schematic of the three-disk HDD spindle system.

the vibration of which must be precisely controlled. The purpose of this paper is to employ a substructure synthesis technique [10] to investigate the longitudinal coupled vibrations of a flexible shaft with multiple flexible disks. The method is computationally efficient and easy to use, and does not need the large number of degrees of freedom as required in finite element analysis. As illustrative examples, computer hard disk drive spindle systems used in commercial personal computers are analyzed by the method formulated in this paper.

2. THEORETICAL ANALYSIS

2.1. SYSTEM DESCRIPTION

Consider an analysis model consisting of a flexible shaft and M identical flexible disks rigidly attached to the shaft, as shown in Figure 2. The shaft is a hollow beam with varying

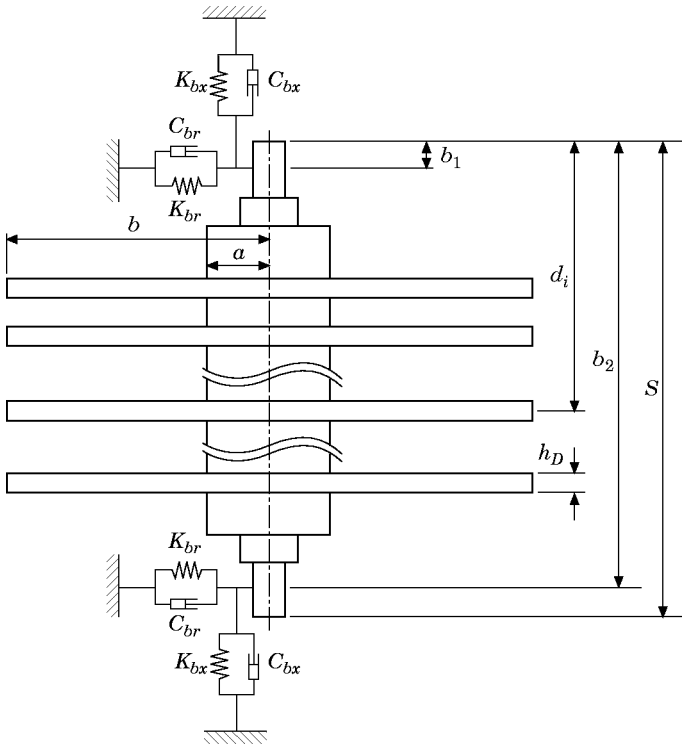

Figure 2. Analysis model.

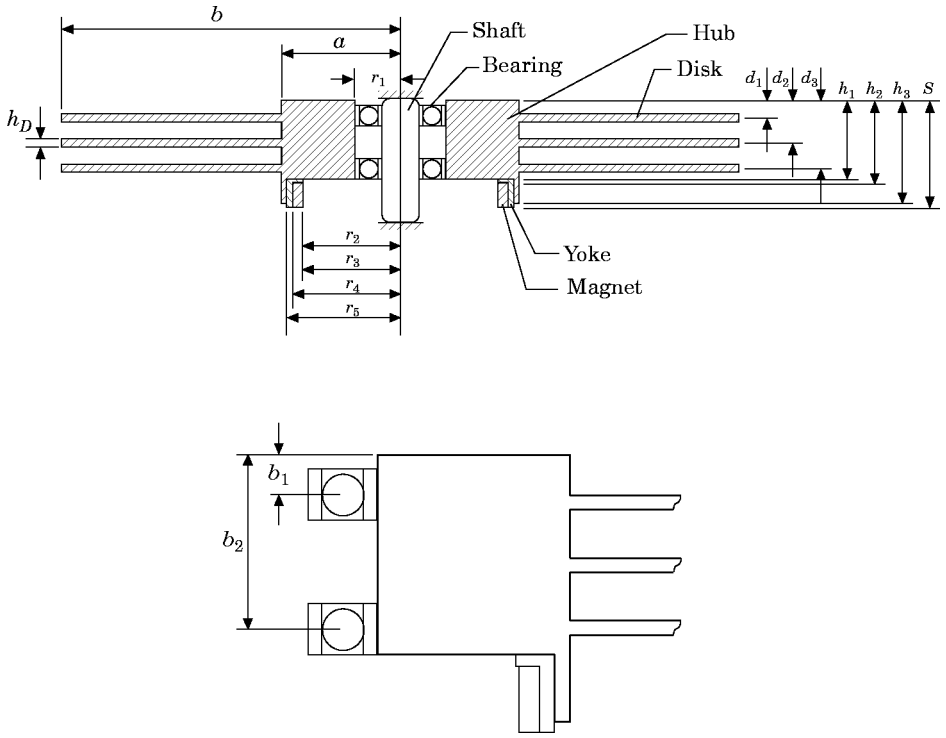

Figure 3. Cross-sectional view of the simulation model.

annular cross-section and varying material properties. It is assumed that plane cross-sections of the shaft remain plane during deformation and that the particles in every cross-section move only in the axial direction of the shaft. The effects of lateral displacements upon the longitudinal motions are neglected. Note that the shaft here consists of the hub, clamp, spacer, clamped parts of disks, magnet and yoke as shown in Figure 1.

Each disk is a uniform circular plate. The classical thin plate theory is used to describe the disk vibration, where the non-linear effect and the thick plate effects of rotary inertia and shearing deformation are neglected. The centrifugal stiffening effect of the disk is included. In addition, small deformation is assumed throughout the analysis. The complicated longitudinal coupled vibrations of the flexible disks/shaft system will be analyzed. In particular, a few lowest vibrational modes are of major interest.

2.3. ANALYSIS METHOD

A substructure synthesis technique is used to investigate the longitudinal coupled vibrations. The total system is regarded as a disconnected assemblage of substructures (flexible shaft and flexible disks) which satisfy the constraint conditions of motion on the disconnected points. The energy elements for every substructure are determined by elastic deformations and fictitious constraint conditions. The motion of every substructure is represented as a finite series of weighted admissible functions. As admissible functions, the mode shapes obtained from the analytical solutions of individual non-rotating elements can be used. The energy elements are obtained in a discretized form by expressing motions

in terms of weighted admissible functions. Then, the Lagrange's equations are used to formulate the equations of motion. A computer program is developed to simulate the natural frequencies and mode shapes of the longitudinal coupled vibrations.

2.3. ENERGY FUNCTIONS

For the longitudinal coupled vibrations of the shaft and disk umbrella modes, only longitudinal displacements need to be considered, and no gyroscopic moments and rotary inertia effect exist. The longitudinal displacement of the shaft is denoted by $u(x, t)$ and the transverse displacement of the disk relative to the flat disk position is denoted by $w(r, \theta, t)$. The positive directions of $u(x, t)$ and $w(r, \theta, t)$ are downwards in Figure 2.

The potential (strain) energy of the shaft is

$$V_S(t) = \tfrac{1}{2} \int_0^S E_S A_S(x) \left[\frac{\partial u(x, t)}{\partial x} \right]^2 \mathrm{d}x, \tag{1}$$

where S is the length of the shaft, E_S is the Young's modulus, $A_S(x)$ is the variable cross-sectional area, and $E_S A_S$ denotes the stiffness of the shaft. The assumption made here is that displacements, strains and stresses are uniform at a given cross-section, implying that plane cross-sections remain plane during deformation. Under the same assumption, the kinetic energy simply becomes

$$T_S(t) = \tfrac{1}{2} \int_0^S \rho_S A_S(x) \left[\frac{\partial u(x, t)}{\partial t} \right]^2 \mathrm{d}x, \tag{2}$$

where ρ_S is the mass per unit volume of the shaft. Note that the energies associated with the rigid body rotation are neglected since they will subsequently be cancelled out in the Lagrange's equations.

Considering the geometric compatibility conditions between two substructures, the kinetic energy of the ith disk ($i = 1, 2, \ldots, M$) can be written as

$$T_{Di}(t) = \frac{\rho_D h_D}{2} \int_0^{2\pi} \int_a^b (\dot{w} + \dot{u}_{di})^2 r \, \mathrm{d}r \, \mathrm{d}\theta, \tag{3}$$

where a and b are the inner-clamping radius and the outer radius of the disk respectively, ρ_D is the mass per unit volume of the disk, h_D is the disk thickness and u_{di} is the shaft longitudinal displacement at the ith disk location. The symbol " $\bullet$ " denotes differentiation with respect to time, $\partial/\partial t$. The potential energy of the disk includes two parts [11]. First, the potential energy due to pure bending:

$$V_{D1i}(t) = \frac{D}{2} \int_0^{2\pi} \int_a^b \left\{ (\nabla^2 w_i)^2 - 2(1 - \nu_D) \frac{\partial^2 w_i}{\partial r^2} \left(\frac{1}{r} \frac{\partial w_i}{\partial r} + \frac{1}{r^2} \frac{\partial^2 w_i}{\partial \theta^2} \right) \right.$$

$$\left. + 2(1 - \nu_D) \left[\frac{\partial}{\partial r} \left(\frac{1}{r} \frac{\partial w_i}{\partial \theta} \right) \right]^2 \right\} r \, \mathrm{d}r \, \mathrm{d}\theta, \tag{4}$$

where ν_D is the Poisson's ratio, ∇^2 is the Laplacian operator, D is the flexural rigidity and E_D is the Young's modulus. Appendix A summarizes the detailed expressions. Second, the potential energy due to the additional stretching of the middle plane caused by transverse

displacements $w(r, \theta, t)$ in the presence of in-plane centrifugal stresses:

$$V_{D2i}(t) = \tfrac{1}{2}\int_0^{2\pi}\int_a^b \left[N_r\left(\frac{\partial w_i}{\partial r}\right)^2 + \frac{N_\theta}{r^2}\left(\frac{\partial w_i}{\partial \theta}\right)^2\right] r \, \mathrm{d}r \, \mathrm{d}\theta, \tag{5}$$

where N_r and N_θ are stress resultants, and their expressions are given in Appendix A where Ω is the constant rotating speed of the spindle. In the following discussion of small deflections, N_r and N_θ are considered to remain unchanged. Since the stresses are distributed symmetrically about the axis of rotation for a perfect disk, shear stresses vanish, i.e., $N_{r\theta} = 0$. The total kinetic and potential energy of the disks are given by

$$T_D = \sum_1^M T_{Di}, \qquad V_D = \sum_1^M (V_{D1i} + V_{D2i}). \tag{6a, b}$$

The strain energy and the Rayleigh's dissipation function of the two rolling-element bearings are

$$V_B = \tfrac{1}{2}K_{Bx}(u_{b1}^2 + u_{b2}^2), \qquad \text{and} \qquad F_B = \tfrac{1}{2}C_{Bx}(\dot{u}_{b1}^2 + \dot{u}_{b2}^2), \tag{7}$$

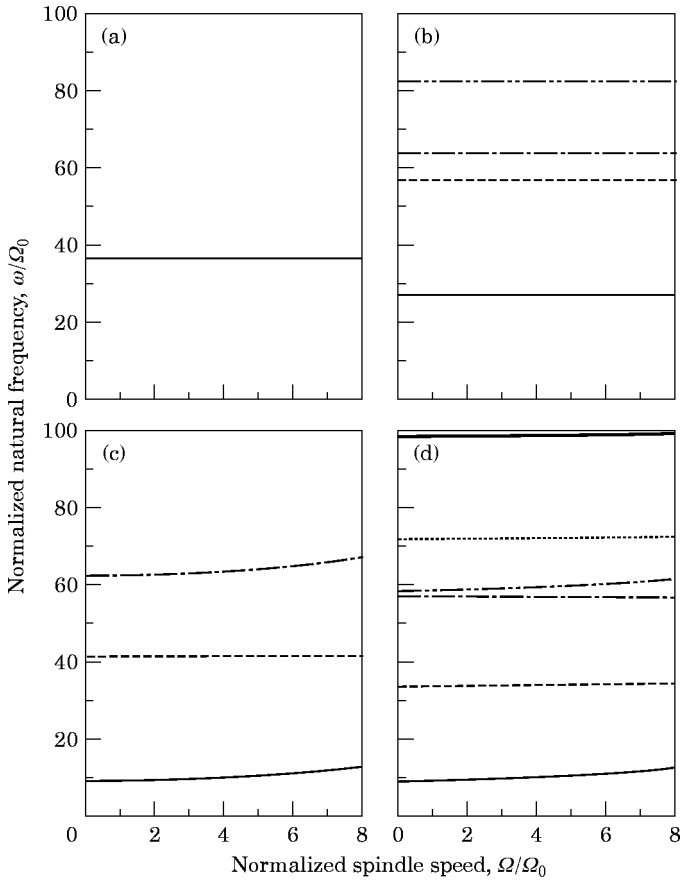

Figure 4. Natural frequencies of the longitudinal coupled vibrations of the one-disk HDD spindle system. (a) Rigid shaft and rigid disk, (b) flexible shaft and rigid disk, (c) rigid shaft and flexible disk, and (d) flexible shaft and flexible disk.

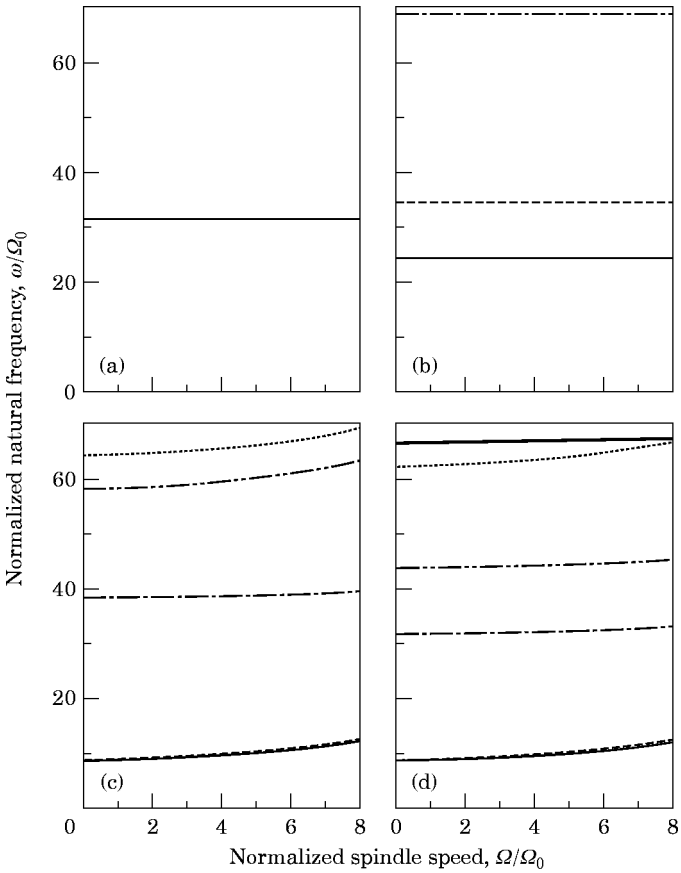

Figure 5. Natural frequencies of the longitudinal coupled vibrations of the two-disk HDD spindle system. (a) Rigid shaft and rigid disks, (b) flexible shaft and rigid disks, (c) rigid shaft and flexible disks, and (d) flexible shaft and flexible disks.

where u_{b1} and u_{b2} are the shaft longitudinal displacements at the locations of two bearings, and K_{Bx} and C_{Bx} are the axial stiffness and damping coefficient of the bearings.

2.4. DISCRETIZATION

As an approximate treatment, the displacements of the continuous shaft and disks will be assumed in the form of a series composed of a linear summation of weighted admissible functions (assumed-modes method). The eigenfunctions of the longitudinal vibration of a free–free rod are chosen as the admissible functions for the shaft. The eigenfunctions of the free vibration of the corresponding stationary disk are chosen as the admissible functions for the disks. Then the shaft longitudinal displacement u and the transverse displacement w_i of the ith disk will take the form

$$u = \mathbf{\Phi}_S \mathbf{Q}_S, \qquad \text{and} \qquad w_i = \mathbf{\Phi}_D \mathbf{Q}_{Di}, \tag{8}$$

where $\mathbf{\Phi}_S$ and $\mathbf{\Phi}_D$ are the row vectors consisting of the admissible functions for the shaft and disks respectively, and $\mathbf{Q}_S$ and $\mathbf{Q}_{Di}$ are the column vectors consisting of the corresponding time-dependent generalized co-ordinates which describe the motions of the shaft and the ith disk respectively. Noting that the zero nodal diameter modes of the disk

are being considered, so no θ dependent variables appear and the modes are not degenerate. From equatons (8), one obtains

$$u_{bi} = \mathbf{\Phi}_S|_{b_i}\mathbf{Q}_S, \qquad \dot{u}_{bi} = \mathbf{\Phi}_S|_{b_i}\dot{\mathbf{Q}}_S, \qquad i = 1, 2,$$
$$u_{dj} = \mathbf{\Phi}_S|_{d_j}\mathbf{Q}_S, \qquad \dot{u}_{dj} = \mathbf{\Phi}_S|_{d_j}\dot{\mathbf{Q}}_S, \qquad j = 1, 2, \ldots, M, \tag{9}$$

where b_i denotes the location of bearing i ($i = 1, 2$) on the shaft, and d_j denotes the location of disk j ($j = 1, 2, \ldots, M$) on the shaft. The locations are measured from the top end of the disks/spindle system (Figure 2). Substitution of equations (8, 9) into equations (1–7) yields the discretized total energy functions as

$$T = T_S + T_D, \qquad V = V_S + V_D + V_B, \qquad F = F_B, \tag{10}$$

where the detailed descriptions are given in Appendix B.

2.5. SYSTEM EQUATIONS OF MOTION

In the last section, the total kinetic, potential energies and the dissipation function have been expressed in terms of a limited number of generalized co-ordinates. Then the Lagrange's equations are ideal for the formulation of the ordinary differential equations

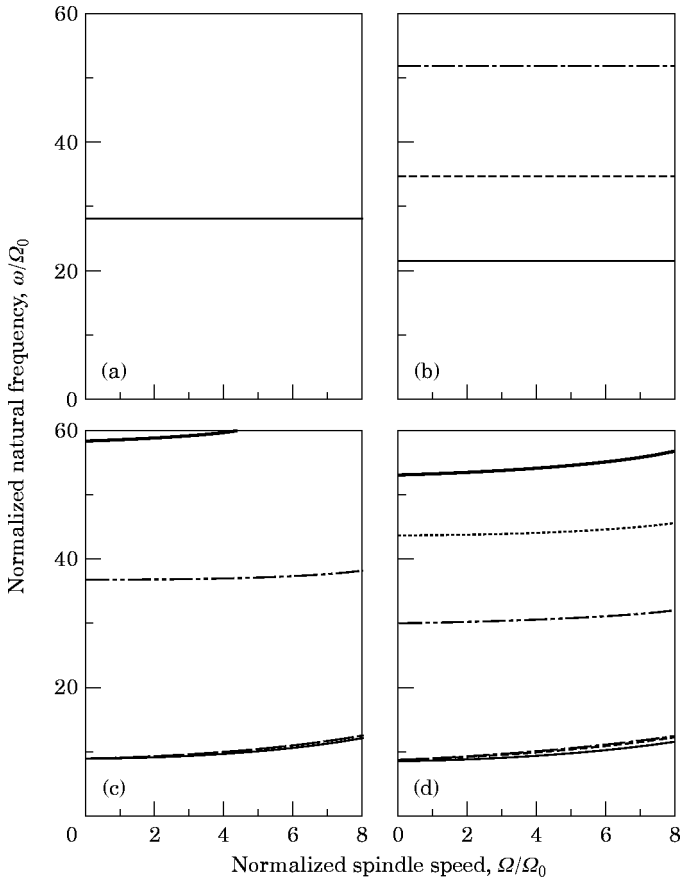

Figure 6. Natural frequencies of the longitudinal coupled vibrations of the three-disk HDD spindle system. (a) Rigid shaft and rigid disks, (b) flexible shaft and rigid disks, (c) rigid shaft and flexible disks, and (d) flexible shaft and flexible disks.

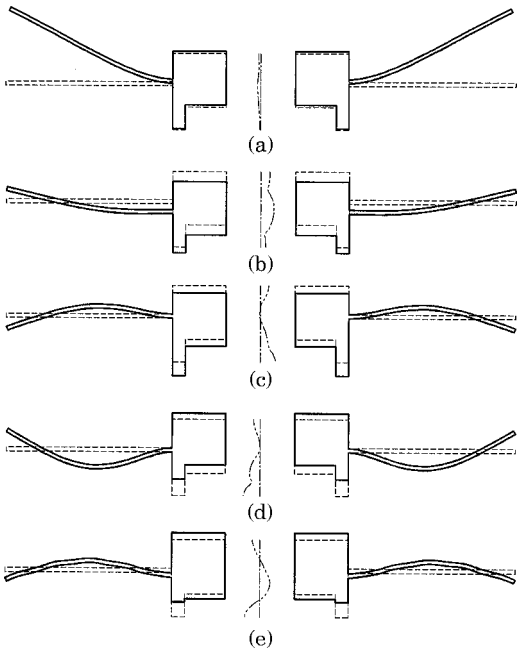

Figure 7. Longitudinal coupled vibration mode shapes of the one-disk HDD spindle system. (a) First, (b) second, (c) third, (d) fourth, and (e) fifth lowest mode.

of motion of the total structure. The Lagrange's equations have the form:

$$(\mathrm{d}/\mathrm{d}t)(\partial L/\partial \dot{\mathbf{q}}_k) - \partial L/\partial \mathbf{q}_k + \partial F/\partial \dot{\mathbf{q}}_k = 0, \tag{11}$$

where $L(=T-V)$, F and $\mathbf{q}_k(\mathbf{Q}_S, \mathbf{Q}_{Di})$ are the Lagrangian, Rayleigh's dissipation function and generalized co-ordinates, respectively. Introducing equation (10) into equation (11) leads to a coupled set of equations:

$$\begin{bmatrix} \mathbf{M}_S & \mathbf{M}_{SD1} & \cdots & \mathbf{M}_{SDM} \\ \mathbf{M}_{SD1}^T & \mathbf{M}_D & 0 & \\ \vdots & 0 & \ddots & \\ \mathbf{M}_{SDM}^T & & & \mathbf{M}_D \end{bmatrix} \begin{Bmatrix} \ddot{\mathbf{Q}}_S \\ \ddot{\mathbf{Q}}_{D1} \\ \vdots \\ \ddot{\mathbf{Q}}_{DM} \end{Bmatrix} + \begin{bmatrix} \mathbf{C}_S & 0 & \cdots & 0 \\ 0 & 0 & 0 & \\ \vdots & 0 & \ddots & \\ 0 & & & 0 \end{bmatrix} \begin{Bmatrix} \dot{\mathbf{Q}}_S \\ \dot{\mathbf{Q}}_{D1} \\ \vdots \\ \dot{\mathbf{Q}}_{DM} \end{Bmatrix}$$

$$+ \begin{bmatrix} \mathbf{K}_S & 0 & \cdots & 0 \\ 0 & \frac{1}{2}(\mathbf{K}_D + \mathbf{K}_D^T) & 0 & \\ \vdots & 0 & \ddots & \\ 0 & & & \frac{1}{2}(\mathbf{K}_D + \mathbf{K}_D^T) \end{bmatrix} \begin{Bmatrix} \mathbf{Q}_S \\ \mathbf{Q}_{D1} \\ \vdots \\ \mathbf{Q}_{DM} \end{Bmatrix} = \begin{Bmatrix} 0 \\ 0 \\ \vdots \\ 0 \end{Bmatrix}, \tag{12}$$

where the element matrices are given in Appendix B. The eigenvalue problem associated with equations (12) can be easily formulated and solved [12].

3. NUMERICAL RESULTS AND DISCUSSION

To demonstrate the proposed method, the commercial HDD spindle systems with one to three disks were selected as illustrative examples. To describe the local deflections of each element, a total of 50 admissible functions (10 for each disk and 20 for shaft

longitudinal defections) were used throughout the simulation. The mode shapes for longitudinal vibration of a rod with free–free boundary condition and transverse vibration of a non-rotating uniform circular plate with inner clamped–outer free boundary condition were used as the admissible functions for the shaft and the disks, respectively.

The simulation model is a short hollow rotating spindle which has one to three identical uniform disks and is simply supported on two ball bearings, as shown in Figure 3. Here, only the three-disk case is shown. For one and two-disk cases, only the disk numbers and disk locations are different. The dimensional data according to Figure 3 are as follows (in mm): $r_1 = 6{\cdot}50$, $r_2 = 14{\cdot}00$, $r_3 = 14{\cdot}10$, $r_4 = 15{\cdot}30$, $r_5 = 16{\cdot}00$, $a = 16{\cdot}50$, $b = 47{\cdot}50$, $h_D = 0{\cdot}80$, $h_1 = 10{\cdot}54$, $h_2 = 11{\cdot}09$, $h_3 = 14{\cdot}14$, $b_1 = 3{\cdot}50$, $b_2 = 12{\cdot}10$, and $S = 14{\cdot}79$. The material and bearing properties are: hub—$E_S = 72{\cdot}0 \times 10^9$ N/m^2, $v_s = 0{\cdot}3$, $\rho_S = 2750$ kg/m^3; disk—$E_D = 72{\cdot}0 \times 10^9$ N/m^2, $v_D = 0{\cdot}36$, $\rho_D = 2800$ kg/m^3; yoke—$E_Y = 204{\cdot}0 \times 10^9$ N/m^2, $v_Y = 0{\cdot}3$, $\rho_Y = 7800$ kg/m^3; magnet—$E_M = 72{\cdot}0 \times 10^9$ N/m^2. $v_M = 0{\cdot}3$, $\rho_M = 5600$ kg/m^3; bearing—$K_{Bx} = 6 \times 10^6$ N/m, $C_{Bx} = 100$ Ns/m. The disk locations for one to three disks HDD systems are separately $d_1 = 5.90$; $d_1 = 2{\cdot}40$, $d_2 = 9{\cdot}40$; and $d_1 = 2{\cdot}40$, $d_2 = 5{\cdot}90$, $d_3 = 9{\cdot}40$. Note that the rotating shaft here consists of the hub, magnet and yoke in Figure 3.

3.1. LONGITUDINAL COUPLED NATURAL FREQUENCIES

The natural frequencies of the HDD spindle systems are shown in Figures 4, 5 and 6. The natural frequencies and rotor speed are normalized by the spindle nominal operating speed, $\Omega_0 = 75$ Hz. The influences of shaft and disk flexibility are included. Figures 4[5 or 6](a), (b), (c) and (d) show the results when both the shaft and the disks are rigid; when the disks are still rigid, but the shaft is flexible; when the shaft is rigid, but the disks are flexible; and when both the shaft and the disks are flexible, respectively. From Figures 4[5 or 6](a) and (b), and Figures 4[5 or 6](a) and (c), one sees that both the shaft and disk

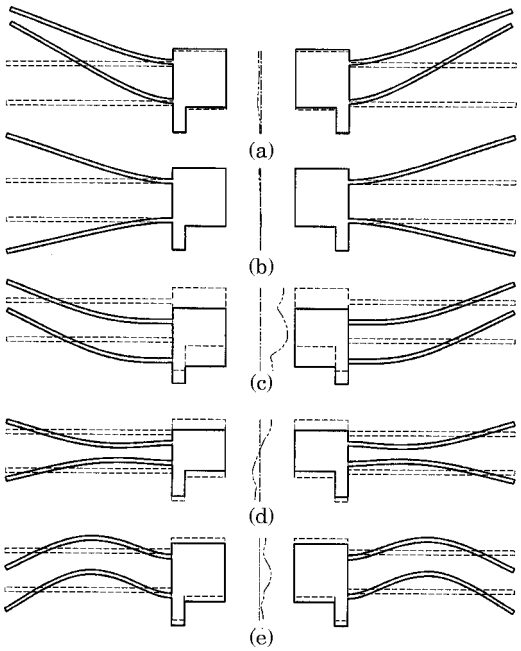

Figure 8. Longitudinal coupled vibration mode shapes of the two-disk HDD spindle system. (a) First, (b) second, (c) third, (d) fourth, and (e) fifth lowest mode.

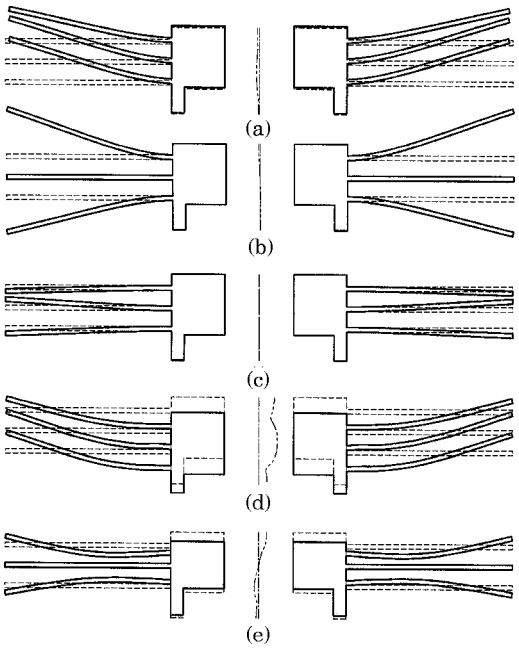

Figure 9. Longitudinal coupled vibration mode shapes of the three-disk HDD spindle system. (a) First, (b) second, (c) third, (d) fourth, and (e) fifth lowest mode.

flexibility have significant influence on the longitudinal coupled vibrations by reducing the values of the natural frequencies and introducing additional natural frequencies. The results in Figure 4[5 or 6](*d*) are used to guide the HDD spindle system design. The effects of centrifugal stiffening are obvious as the rotating speed varied in the figures.

3.2. LONGITUDINAL COUPLED VIBRATIONAL MODES

The five lowest coupled mode shapes are depicted in Figures 7, 8 and 9. The first mode is the disk (0, 0) mode plus the longitudinal translational motion of the assembly as shown in Figure 7[8 or 9](*a*) (bouncing mode). Here disk (m, n) mode is referred to as the disk mode with m nodal diameters and n nodal circles. Note that only the disk modes with zero nodal diameter give contribution to the longitudinal coupled motion. This is due to the net inertia force produced by the umbrella modes of the disk [1]. This force causes the interaction between the disks and the spindle, leading to change in system natural frequencies and mode shapes. The inertia force is canceled out for k-nodal diameter disk modes ($k \neq 0$) and thus no such interaction will be found. In case of the first coupled mode (Figure 7[8 or 9](*a*)), the in-phase mode shapes of the disk(s) tend to intensify the net inertia force to the shaft so that the longitudinal motion of the system is easily induced. Figures 4[5 or 6](*b*) and (*d*) indicate that the disk flexibility will significantly lower the coupled modal frequency with the shaft longitudinal translational mode.

On the other hand, the out-of-phase mode shapes of the two and three disks tend to nullify the net inertia force for the second coupled mode in Figure 8 and the second and third coupled modes in Figure 9. These modes are called balanced disk modes. In fact, these modes can be well predicted from the individual flexible disk analysis without considering the shaft and bearing flexibility. The natural frequencies corresponding to the second and third coupled modes in Figure 9 cannot be separated from one another in Figure 6(*c*).

The second mode in Figure 7, the third mode in Figure 8, and the fourth mode in Figure 9 have the disk flexural motion plus the translational motion of the assembly. Each element has the local mode shape similar to that of the first mode but the motions associated with the spindle and the disks are now out-of-phase.

Modes (c)–(e) in Figure 7, modes (d) and (e) in Figure 8, and mode (e) in Figure 9 are associated with the shaft flexible modes and the disk (0, 1) mode.

4. CONCLUSIONS

A substructure synthesis technique has been developed to investigate the complex longitudinal coupled vibrations of the flexible shaft–multiple flexible disk systems. The following conclusions can be drawn for the HDD spindle systems from the investigation.

(1) The longitudinal coupled natural frequencies are significantly influenced by both the disk flexibility and the shaft flexibility.

(2) For the practically interesting modes (mode (a) in Figure 7, modes (a) and (b) in Figure 8, and modes (a)–(c) in Figure 9), the main effect of disk flexibility is in reducing the natural frequency of the longitudinal translational mode (bouncing mode) and introducing additional balanced disk modes.

REFERENCES

1. C. W. Lee, H. S. Jia, C. S. Kim and S. B. Chun 1997 *Journal of Sound and Vibration* (accepted for publication). Tuning of simulated natural frequencies for a flexible shaft–multiple flexible disk system.
2. J. A. Dopkin and T. E. Shoup 1974 *American Society of Mechanical Engineers Journal of Engineering for Industry* **96**, 1328–1333. Rotor resonant speed reduction caused by flexibility of disks.
3. D. R. Chivens and H. D. Nelson 1975 *American Society of Mechanical Engineers Journal of Engineering for Industry* **97**, 881–886. The natural frequencies and critical speeds of a rotating, flexible shaft-disk system.
4. N. Klompas 1978 *American Society of Mechanical Engineers Journal of Engineering for Power* **100**, 647–654. Significance of disk flexing in viscous-damped jet engine dynamics.
5. F. J. Wilgen and A. L. Schlack 1979 *American Society of Mechanical Engineers Journal of Mechanical Design* **101**, 298–303. Effects of disk flexibility on shaft whirl stability.
6. A. A. S. Shahab and J. Thomas 1987 *Journal of Sound and Vibration* **114**, 435–452. Coupling effects of disc flexibility on the dynamic behaviour of multi disc-shaft systems.
7. G. T. Flowers and F. Wu 1996 *American Society of Mechanical Engineers Journal of Vibration and Acoustics* **118**, 204–208. Disk/shaft vibration induced by bearing clearance effects: analysis and experiment.
8. S. B. Chun and C. W. Lee 1996 *Journal of Sound and Vibration* **189**, 587–608. Vibration analysis of shaft-bladed disk system by using substructure synthesis and assumed modes method.
9. C. W. Lee and S. B. Chun 1997 *American Society of Mechanical Engineers Journal of Vibration and Acoustics* **119**. Vibration analysis of a rotor with multiple flexible disks using assumed modes method.
10. L. Meirovitch 1980 *Computational Methods in Structural Dynamics*. The Netherlands: Sijthoff & Noordhoff; pp. 298–300 and 401–409.
11. H. S. Jia and C. W. Lee 1997 *Proceedings of the Second International Conference on Hydrodynamic Bearing-Rotor System Dynamics*, *Xi' an*, *China*, 199–204. Effects of imperfections in a rotating circular disk on its vibration characteristics.
12. C. W. Lee 1993 *Vibration Analysis of Rotors*. The Netherlands: Kluwer Academic Publishers; pp. 156–159.

APPENDIX A: STRESSES; LAPLACIAN OPERATOR; AND FLEXURAL RIGIDITY

$$N_r = \frac{\rho_D h_D \Omega^2}{8}\left[-(3+v_D)r^2 + C_1 + C_2\frac{1}{r^2}\right],$$

$$N_\theta = \frac{\rho_D h_D \Omega^2}{8}\left[-(1+3v_D)r^2 + C_1 - C_2\frac{1}{r^2}\right],$$

$$C_1 = \frac{(1+v_D)(3+v_D)b^4 + (1-v_D^2)a^4}{(1+v_D)b^2 + (1-v_D)a^2}, \qquad C_2 = b^2a^2\frac{(1-v_D)(3+v_D)b^2 - (1-v_D^2)a^2}{(1+v_D)b^2 + (1-v_D)a^2},$$

$$\nabla^2 = \partial^2/\partial r^2 + \partial/(r\partial r) + \partial^2/(r^2\partial\theta^2), \qquad D = E_D h_D^3/[12(1-v_D^2)].$$

APPENDIX B: DISCRETIZED TOTAL ENERGY FUNCTIONS

$$T = T_S + T_D = \tfrac{1}{2}\dot{\mathbf{Q}}_S^{\mathrm{T}} M_S \dot{\mathbf{Q}}_S + \tfrac{1}{2}\sum_{i=1}^{M} \dot{\mathbf{Q}}_{Di}^{\mathrm{T}} M_D \dot{\mathbf{Q}}_{Di} + \sum_{i=1}^{M} \dot{\mathbf{Q}}_S^{\mathrm{T}} M_{SDi} \dot{\mathbf{Q}}_{Di},$$

$$V = V_S + V_D + V_B = \tfrac{1}{2}\mathbf{Q}_S^{\mathrm{T}} K_S \mathbf{Q}_S + \tfrac{1}{2}\sum_{i=1}^{M} \mathbf{Q}_{Di}^{T} K_D \mathbf{Q}_{Di}, \qquad F = F_B = \tfrac{1}{2}\dot{\mathbf{Q}}_S^{\mathrm{T}} C_S \dot{\mathbf{Q}}_S,$$

where

$$\mathbf{M}_S = \int_0^S \rho_S A_S \mathbf{\Phi}_S^{\mathrm{T}} \mathbf{\Phi}_S \,\mathrm{d}x + m_{D0}\sum_{i=1}^{M} \mathbf{\Phi}_S|_{d_i}^{\mathrm{T}} \mathbf{\Phi}_S|_{d_i}, \qquad \mathbf{M}_D = 2\pi\rho_D h_D \int_a^b \mathbf{\Phi}_D^{\mathrm{T}} \mathbf{\Phi}_D r \,\mathrm{d}r,$$

$$\mathbf{M}_{SDi} = 2\pi\rho_D h_D \mathbf{\Phi}_S^{\mathrm{T}}|_{d_i} \int_a^b \mathbf{\Phi}_D r \,\mathrm{d}r,$$

$$\mathbf{K}_S = \int_0^S E_S A_S \mathbf{\Phi}_S'^{\mathrm{T}} \mathbf{\Phi}_S' \,\mathrm{d}x + K_{Bx}(\mathbf{\Phi}_S|_{b_1}^{\mathrm{T}} \mathbf{\Phi}_S|_{b_1} + \mathbf{\Phi}_S|_{b_2}^{\mathrm{T}} \mathbf{\Phi}_S|_{b_2}),$$

$$\mathbf{K}_D = 2\pi\int_a^b [Dr\mathbf{\Phi}_{\mathrm{D}}''^{\mathrm{T}}\, \mathbf{\Phi}_D'' + 2Dv\mathbf{\Phi}_D''^{\mathrm{T}} \mathbf{\Phi}_D' + (N_r r + D/r)\mathbf{\Phi}_D'^{\mathrm{T}} \mathbf{\Phi}_D'] \,\mathrm{d}r,$$

$$\mathbf{C}_s = C_{Bx}(\mathbf{\Phi}_S|_{b_1}^{\mathrm{T}}\, \mathbf{\Phi}_S|_{b_1} + \mathbf{\Phi}_S|_{b_2}^{\mathrm{T}}\, \mathbf{\Phi}_S|_{b_2}),$$

where primes $''$ represent differentiations with respect to the spatial variables x and r for $\mathbf{\Phi}_S$ and $\mathbf{\Phi}_D$, respectively, and m_{D0} is the mass of a disk.

APPENDIX C: NOMENCLATURE

a	disk inner-clamping radius
A_S	cross-sectional area of the shaft
b	disk outer radius
b_i	locations of bearings on the shaft
C_{Bx}	axial damping coefficient of bearings
D	flexural rigidity of the disk
d_i	locations of disks on the shaft

E	Young's modulus
F	Rayleigh's dissipation function
h_D	thickness of the disk
K_{Bx}	axial stiffness of bearings
L	Lagrangian
M	total number of disks
m_{D0}	mass of a disk
(m, n)	disk mode with m nodal diameters and n nodal circles
N_r, N_θ	stress resultants
$\mathbf{q}_k, \mathbf{Q}_{Di}, \mathbf{Q}_S$	generalized co-ordinates
(r, θ)	polar co-ordinates for a disk
S	length of the shaft
T	kinetic energies
u, u_{bi}, u_{di}	longitudinal displacements of the shaft
V	potential energies
w, w_i	transverse displacements of disks
$\mathbf{\Phi}_D, \mathbf{\Phi}_S$	row vectors consisting of admissible functions
ρ	mass per unit volume
v	Poisson's ratio
$\mathbf{V}^2$	Laplacian operator
Ω	rotational speed of the shaft
Ω_0	nominal operating speed of the spindle

Subscripts

B	bearing
b_i, d_i	values evaluated at the ith bearing and ith disk location
D	disk
D_i	ith disk
M	magnet
S	shaft (hub)
Y	yoke